X-RAY SPECTROMETRY
*X-Ray Spectrom.* 2003; **32**: 307–311
Published online in Wiley InterScience (www.interscience.wiley.com). DOI: 10.1002/xrs.643

XRS

# Comparison between intensity jumps in experimental, simulated and theoretical multielemental spectra

**R. Figueroa,[1]* M. García[1] and D. Brusa[2]**

[1] Physical Sciences Department, Engineering, Sciences and Management Faculty, Universidad de La Frontera, Avenida Francisco Salazar, 01145 Temuco, Chile
[2] Mathematics, Astronomy and Physics Faculty (FaMAF), Universidad Nacional de Córdoba, Córdoba, Argentina

Received 8 May 2002; Accepted 22 January 2003

**The results obtained by applying the theory developed for the SEICXRF method and applying a Monte Carlo simulation code (MCS) are compared with the experimental data in order to validate this theory. Specifically, an assay is made with the spectra corresponding to a brass sample and a soil sample. The experimental data were corrected considering the chamber efficiency and the dead time of the detection system. The considerations taken into account in order to obtain a correct comparison between theory and experiment are discussed in detail. Good agreement between spectra is observed, taking as reference the given values of the elemental composition. The experimental intensity jumps are in agreement with those predicted by the theory and by the MCS. Copyright © 2003 John Wiley & Sons, Ltd.**

## INTRODUCTION

One way to validate the developed algorithms of the fundamental parameters to determine the intensity jump in the selective excitation and integral counting of x-ray fluorescence (SEICXRF) method is through a comparison of a spectrum obtained directly from the theory with that obtained by Monte Carlo simulation (MCS), contrasting the latter with those obtained from experiment.

In order to validate these comparisons, it is fundamental that each condition must be very similar in every stage; otherwise, it is necessary to know the corrections to be introduced to compensate for the differences that could exist. The main objective of this study was to prove the agreement between the theory, the MCS and the experiment.

The elemental compositions of the analyzed samples, measured through other analytical techniques, were as follows: standard brass sample, C26000 = Cu(0.7) + Zn(0.3) and reference soil sample, R14 (measured by conventional wet chemical analysis) = $Al_2O_3$ (0.1501) + $SiO_2$ (0.6955) + $Fe_2O_3$ (0.0482) + MnO (0.00067) + MgO (0.0096) + CaO (0.0106) + $Na_2O$ (0.0233) + $K_2O$ (0.0224) + $TiO_2$ (0.0074). The R14 values were transformed to elemental concentrations.

## THEORY

This stage implies the calculation of the emitted radiation by the source for each material sample when this is excited by a quasi-monochromatic flux. The algorithm to calculate the spectrum due to the primary fluorescence $I_P(\lambda)$[1,2] is given by

$$I_P(\lambda) = I(\lambda)\frac{\Delta\Omega}{4\pi}\csc\psi_1 \sum_i \sum_q \sum_u C_i \omega_i^q \tau_i^q(\lambda) \frac{f_j^{q,u}}{\mu_s'(\lambda) + \mu_s''(\lambda_i^{q,u})} \quad (1)$$

where $\mu_s'(\lambda) = \mu_s(\lambda)\csc\psi_1$ and $\mu_s''(\lambda) = \mu_s(\lambda_i^{q,u})\csc\psi_2$ and

$I(\lambda)$ = flux intensity of the incident beam to the energy $E = E(\lambda)$;
$C_i$ = concentration of element $i$;
$\mu_s(\lambda_i^{q,u})$ = mass absorption coefficient at the energy of the characteristic line, $u$;
$\mu_s(\lambda)$ = mass absorption coefficient at the incident energy, $E(\lambda)$;
$\tau_i^q(\lambda)$ = net photoelectric absorption coefficient of edge $q$ of element $i$ for each $\lambda$;
$f_i^{q,u}$ = line fraction of the characteristic line, $u$, at edge $q$ of element $i$;
$\omega_i^q$ = fluorescence yield at edge $q$ of element $i$.

As the algorithm considers the contribution of all the generated fluorescent intensity starting from an excitation energy, $E(\lambda)$, then, the fluorescence background fall on each edge is considered for Eqn (1). For the secondary fluorescence spectrum, the following expression was used:[1]

$$I_s(\lambda) = I_0(\lambda)\frac{\Delta\Omega}{4\pi}\csc\psi_1 \sum_i \sum_u \sum_r \sum_v \sum_{j\neq i} \frac{C_i\omega_i^q\tau_i^q(\lambda)}{2} \times \frac{D_{i,j}^{q,r} C_j \omega_j^r \tau_j^r f_j^{r,v} f_i^{q,u} P_{i,j}}{\mu_s'(\lambda) + \mu_s''(\lambda_j^{r,v})} \quad (2)$$

where

$$P_{i,j} = \frac{1}{\mu_s(\lambda_i^q)} \ln\left[1 + \frac{\mu_s(\lambda_i^q)}{\mu_s'(\lambda_i^{q,u})}\right] + \frac{1}{\mu_s(\lambda_j^{r,v})} \ln\left[1 + \frac{\mu_s''(\lambda_j^{r,v})}{\mu_s'(\lambda_i^{q,u})}\right]$$

*Correspondence to: R. Figueroa, Physical Sciences Department, Engineering, Sciences and Management Faculty, Universidad de La Frontera, Avenida Francisco Salazar, 01145 Temuco, Chile.
E-mail: rodolfof@ufro.cl
Contract/grant sponsor: Universidad de La Frontera.

$$\text{and } D_{i,j}^{q,r} = \begin{cases} 1 & if \quad \lambda_j^{r,v} \geq \lambda_i^{q,u} \\ 0 & if \quad \lambda_j^{r,v} < \lambda_i^{q,u} \end{cases}$$

The numerical calculation considers a constant intensity for each exciting energy and includes the factors that take into account the absorption by the air and by the detector window for each of them. Then, the Eqns (1) and (2) become

$$I_P(\lambda) = I_0(\lambda)\frac{\Delta\Omega}{4\pi}\csc\psi_1 \sum_i \sum_q \sum_u C_i\omega_i^q\tau_i^q(\lambda) \times \frac{f_i^{q,u}\exp\{\mu_A(\lambda_i^{q,u})\rho_A d_{SD} + \mu_{Be}(\lambda_i^{q,u})\rho_{Be}s_{WBe}\}}{\mu_s'(\lambda) + \mu_s''(\lambda_i^{q,u})} \quad (3)$$

and

$$I_s(\lambda) = I_o(\lambda)\frac{\Delta\Omega}{4\pi}\csc\psi_1 \sum_i \sum_u \sum_r \sum_v \sum_{j\neq i} \frac{C_i\omega_i^q\tau_i^q(\lambda)}{2} \times \frac{D_{i,j}^{q,r}C_j\omega_j^r\tau_j^r f_j^{r,v} f_i^{q,u} P_{i,j}}{\mu_s'(\lambda) + \mu_s''(\lambda_j^{r,v})} \times \exp\{\mu_A(\lambda_j^{r,v})\rho_A d_{SD} + \mu_{Be}(\lambda_j^{r,v})\rho_{Be}s_{WBe}\} \quad (4)$$

where

$\mu_A(\lambda_i^{q,u})$ = air absorption coefficient at the characteristic energy of element $i$;
$\mu_A(\lambda_j^{r,v})$ = air absorption coefficient at the characteristic energy of element $j$;
$\rho_A$ = air density;
$d_{SD}$ = sample–detector distance;
$\mu_{Be}(\lambda_j^{q,u})$ = beryllium absorption coefficient at the characteristic energy of element $i$;
$\mu_{Be}(\lambda_j^{r,v})$ = beryllium absorption coefficient at the characteristic energy of element $j$;
$\rho_{Be}$ = beryllium density;
$S_{WBe}$ = thickness of the beryllium window.

A 45° geometry is considered for the characteristic photons without angular dispersion. This means that all photons arrive parallel to the detector. A 100% detection efficiency is also assumed, so that the detector counts all photons.

## MONTE CARLO SIMULATION (MCS)

The MCS code used in this work is called PENELOPE (Penetration Energy Loss of Positrons and Electrons), which has been specially adapted for photons, showing a good behavior in characteristic x-ray simulations.[3] The MCS process requires the creation of a virtual sample whose elemental composition is equal to that considered by the theory and the most similar to the real one.

PENELOPE does not consider either the molecular composition or the crystalline structure of the sample, so this is considered as an amorphous and homogeneous material. The molecular composition could cause oscillations in the absorption edge top.[4] However, this effect could be adequately compensated in order to determine the jump intensity that happens at an edge.[1] A block scheme is presented in Fig. 1, which describes the whole MCS process.

The MCS conditions are very similar to those considered by the theory, but these are also closer to the experimental conditions, because a quasi-monochromatic incident beam is considered and the characteristic photons have an angular dispersion defined by the detection cone. The number of simulated incident photons was $10^6$

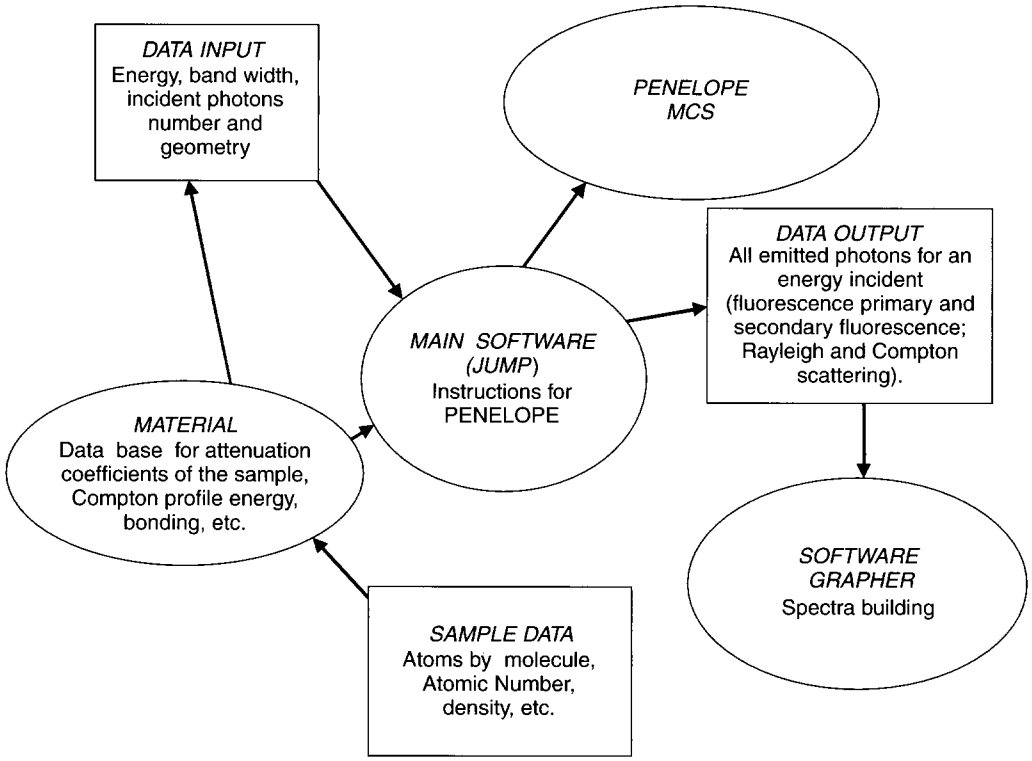


**Figure 1.** Scheme of the Monte Carlo simulation (MCS) process.

for every incident energy. The number of emitted photons in each fluorescent jump is considerably reduced by the physical phenomena involved in a determined sample and by the detection geometry used. In addition, the MCS allows us to include all radiation emitted by the sample (primary and secondary fluorescence, single and multiple dispersion).

## THEORY AND MCS COMPARISON

In this stage, the results obtained by theory [Eqns (1) and (2)] and by MCS were compared, without considering the attenuation (air path and Be window). The intensities are normalized to the values given by MCS. Figures 2 and 3 present the spectra corresponding to a binary sample C26000 and a multielemental sample R14. Figure 2 presents the superposition of the spectra associated with the C26000 sample, where the copper jump intensity is the same (there is no fluorescent background) with no contribution of the dispersion, which was almost the same all over the spectrum. In this case, the ratios of jumps, $h_{Cu}/h_{Zn}$, are equal to 6.18 and 6.38 for theory and MCS, respectively, showing a relative difference between theory and MCS of 3.2%.

Analogously, Figure 3 shows the superposition of the spectra associated with the R14 sample. In this case, the total intensity is normalized to the intensity at the Ti edge (jump + fluorescent background). Table 1 presents the results of the comparison between the jumps associated with the C26000 sample, comparing the sum of the fluorescent contributions with the MCS results. Table 2 presents the results for the R14 sample.

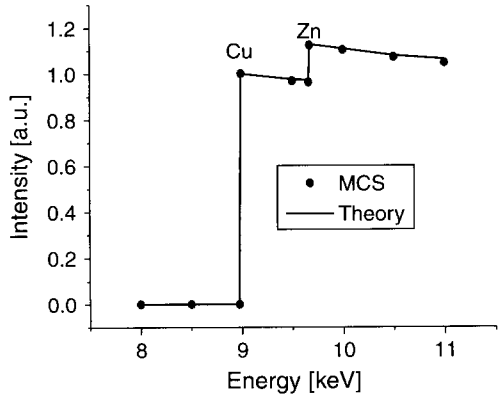


**Figure 2.** Superposition of theoretical and MCS spectra associated with the C26000 sample, in vacuum.

## EXPERIMENTAL

A basic experimental setup of an SEICXRF spectrometer in a synchrotron light line[5] is presented in Fig. 4. It has the same geometry of the preceding stages with a monochromator, an ionization chamber, a sample and a detector. The associated electronics for each of these devices are not shown. It is necessary to introduce some correction factors, which are not considered either in the theory or in the MCS; these factors are related to the efficiency of the ionization chamber, the chamber–sample path attenuation and the dead time associated with the detection system. Once that the chamber efficiency correction and the attenuation correction by the air path have been copied out, the incident beam is obtained. Subsequently, the dead time corrections are carried out to obtain the measured spectrum.

**Table 1.** Comparison between the jumps determined by theory (A + B) and Monte Carlo simulation MCS (M) for the binary sample C26000[a]

| Element | Theory (A) primary | Theory (B) secondary | Theory (T) (A + B) | MCS (M) (normalized) | MCS (M) [counts] | Total difference MCS − theory (M − T)/M | Statistical error MCS $\sqrt{M}/M$ |
|---|---|---|---|---|---|---|---|
| Cu | 1 | 0 | 1 | 1 | 3452 | 0 | 0.0171 |
| Zn | 0.149 | 0.013 | 0.162 | 0.157 | 541 | −0.0318 | 0.0415 |

[a] Columns A and B show the jumps due to the primary and the secondary fluorescences obtained by theory, respectively. The differences between theory (T) and normalized MCS (M) and their comparison with the statistical error are presented in the last two columns. The intensity jumps were normalized with respect to the Cu jump.

**Table 2.** As Table 1 but for the R14 multielemental sample (the intensity jumps were normalized respect to the Fe jump obtained from MCS)

| Element | Theory (A) primary | Theory (B) secondary | Theory (T) (A + B) | MCS (M) (normalized) | MCS (M) [counts] | Total difference MCS − theory (M − T)/M | Statistical error MCS $\sqrt{M}/M$ |
|---|---|---|---|---|---|---|---|
| Al | 0.1256 | 0.0000 | 0.1256 | 0.1318 | 346 | 0.0462 | 0.0530 |
| Si | 0.4589 | 0.0019 | 0.4608 | 0.4707 | 1236 | 0.0251 | 0.0284 |
| K | 0.1157 | 0.0015 | 0.1173 | 0.1074 | 282 | −0.0922 | 0.0595 |
| Ca | 0.0541 | 0.0004 | 0.0545 | 0.0548 | 144 | 0.0069 | 0.0833 |
| Ti | 0.0545 | 0.0003 | 0.0548 | 0.0559 | 147 | 0.0204 | 0.0824 |
| Mn | 0.0129 | 0.0004 | 0.0133 | 0.0101 | 27 | −0.297 | 0.190 |
| Fe | 0.9885 | 0.0046 | 0.9931 | 1.0000 | 2626 | 0.0068 | 0.0195 |

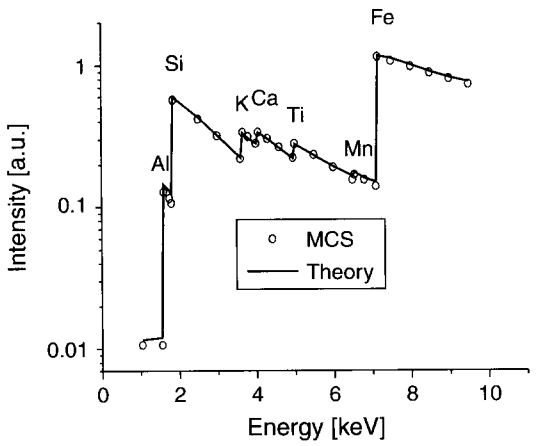


**Figure 3.** Superposition of theoretical and MCS spectra associated with the R14 sample, in vacuum.

Finally, with the purpose of obtaining an independent spectrum from the incident intensity, the ratio between the incident and the measured spectra is estimated. Figure 5 shows how the incident original spectrum and the spectrum measured by the detector are modified when the correction factors are applied (example, C26000 sample).

**Table 3.** Comparison between the intensity jumps of the binary sample, C26000, determined by theory (T), by MCS (M) and by experiment (E), with the relative differences between theory and experiment and between MCS and experiment

| Element | Theory (T) | MCS (M) | Experiment (E) | Relative difference (E − T)/E | Relative difference (E − M)/E |
|---|---|---|---|---|---|
| Cu | 1 | 1 | 1 | — | 0 |
| Zn | 0.172 | 0.181 | 0.178 | 0.032 | 0.018 |

## COMPARISON WITH EXPERIMENT

Once the ratio between the corrected incident spectrum and the corrected measured spectrum has been estimated, the definitive spectrum is obtained which is contrasted with a similar one obtained by MCS and with the theoretical spectrum obtained from the sum of Eqns (3) and (4), because the experiment considers the attenuation between the sample and the detector.

Figure 6 presents a comparison between the intensity jumps, normalized to the Cu jump, corresponding to the C26000 sample. Note the similarity between them; the results are shown in Table 3. The ratios of jumps, $h_{Cu}/h_{Zn}$, obtained in this case, are 5.63, 5.82 and 5.53 for the measured,

**Table 4.** As Table 3 but for the R14 multielemental sample, with a new column (differences between laboratories)

| Element | Theory (T) | MCS (M) | Experiment (E) | Relative difference (E − T)/E | Relative difference (E − M)/E | Differences between laboratories[a] (A − B)/B |
|---|---|---|---|---|---|---|
| Ca | 0.0163 | 0.0161 | 0.0152 | 0.0759 | 0.0612 | 0.443 |
| Ti | 0.0328 | 0.0329 | 0.0326 | 0.0064 | 0.0110 | 0.057 |
| Mn | 0.0120 | 0.0119 | 0.0143 | 0.1554 | 0.1606 | 0.343 |
| Fe | 0.9819 | 1 | 1 | 0.0181 | – | 0.131 |

[a] A, laboratory via conventional wet chemical analysis; B, laboratory via ICP.

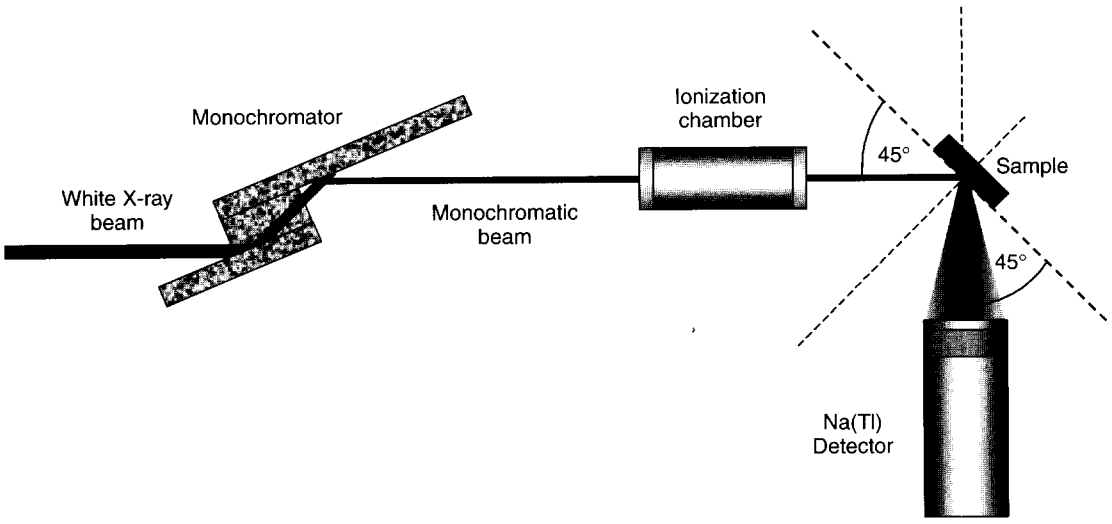


**Figure 4.** Scheme of the experimental setup: a channel cut Si (100) monochromator, a 17 cm long ionizing air chamber and a NaI(Tl) scintillation detector were used. The sample–chamber distance was 10 cm and the detector–sample distance was 11 cm.

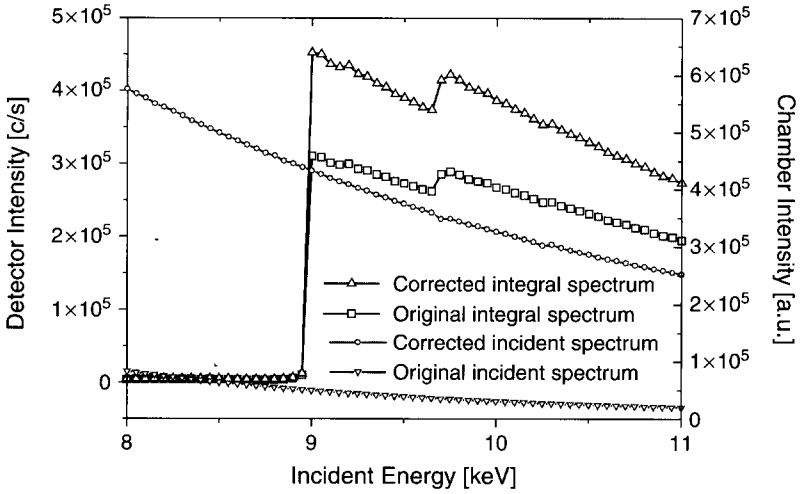


**Figure 5.** Original and corrected integral spectra and original and corrected incident spectra for the C26000 sample.

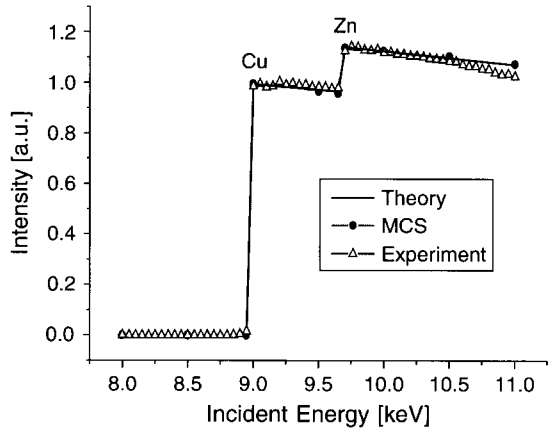


**Figure 6.** Full spectra superposition associated with the C26000 sample, in air.

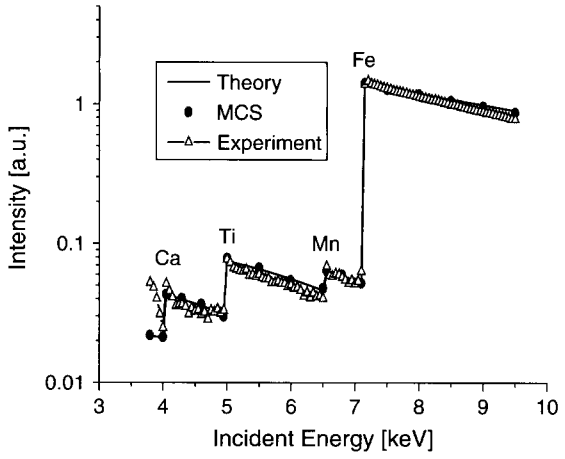


**Figure 7.** Full spectra superposition associated with the R14 sample, in air.

theoretical and simulated jumps, respectively. The last two show differences of −3.3% and 1.8%, respectively, in relation to the first, showing good agreement. Figure 7 presents a comparison for the soil sample, whose results are shown in Table 4. These were normalized to the Fe jump. Note that only four elements appear, since the characteristic lines associated with the elements Al and Si are completely absorbed by the environment, because of the attenuation of the air and the detector window.

## DISCUSSION AND CONCLUSIONS

Comparing the results obtained by the theory and MCS, there are agreements in almost all the intensity jumps determined by each method for the brass and soil samples.

In most of the cases analyzed the differences are lower than the statistical errors, which are determined from the counts obtained by the MCS code. Excellent agreement is obtained for the C26000 brass binary sample. Nevertheless, the agreement was not so good for the R14 soil multielemental sample, because two elements (K and Mn) have slightly larger differences than their corresponding statistical values. In spite of this, we could conclude that there is good agreement in general.

The experimental results show a remarkable agreement with those obtained by the MCS and by the theory. The best agreement is obtained for the C26000 sample; the R14 sample presents some differences, but smaller than those obtained between the laboratories where it was analyzed. Finally, we could conclude that the algorithms and the MCS code developed for the SEICXRF method adequately describe the fluorescence emission phenomenon in the cases analyzed.


### Acknowledgements

The authors express their thanks to those members responsible for the EXAFS line at the National Laboratory of Synchrotron Light, Campinas, Brazil, where most of the measurements were made, to the GEAN Group of the Mathematics, Astronomy and Physics Faculty, Universidad Nacional de Córdoba, Argentina, where the thesis was developed, and to the Universidad de La Frontera, for the financial support to perform this research project.


## REFERENCES


1. Figueroa R. PhD Thesis, Universidad Nacional de Córdoba, 2001.
2. Figueroa R, Riveros A. *Nucleotécnica* 1999; **19**: 19.
3. Salvat F, Fernández JM, Baró J, Sampau J. *PENELOPE*. Informes Técnicos CIEMAT: Barcelona, 1996.
4. Eisenberger P, Kincaid B. *Science* 1978; **200**: 1441.
5. Figueroa R, Riveros A. *Activity Report LNLS* ABTLuS. 1999; **97–98**: 6.7–3.